Ezrin turnover and cell shape changes catalyzed by proteasome in oxidatively stressed cells

TILMAN GRUNE,*,¶ THOMAS REINHECKEL,‡ JAMES A. NORTH,* RUI LI,* PALOMA B. BESCOS,*,[1] RESHMA SHRINGARPURE,* AND KELVIN J. A. DAVIES*,[2]

*Ethel Percy Andrus Gerontology Center and Division of Molecular & Computational Biology, the University of Southern California, Los Angeles, California, USA; ¶Clinics of Physical Medicine and Rehabilitation, Medical Faculty (Charité), Humboldt-University Berlin, Berlin, Germany; and ‡Centre of Surgery and Institute of Clinical Chemistry, Otto von Guericke University Magdeburg, Magdeburg, Germany

ABSTRACT **We find that ezrin, a cytoskeletal protein involved in anchoring actin to the cell membrane, is preferentially degraded and resynthesized after oxidative stress. Ezrin was identified using 2-dimensional gels and amino-terminal microsequencing as one of a select few [^{35}S]methionine prelabeled proteins degraded in clone 9 rat liver cells exposed to hydrogen peroxide (H_2O_2). Metabolic labeling of cellular proteins with [^{35}S]methionine after oxidative stress showed that resynthesis of ezrin rose dramatically but carboxyl terminus anti-ezrin monoclonal antibodies revealed constant intracellular ezrin levels; in other words, degradation and resynthesis were exactly matched. Ezrin degradation was blocked by selective inhibitors of the proteasome (lactacystin, NLVS, and epoxomycin) and by an antisense oligonucleotide directed against the proteasome C2 subunit. H_2O_2 also caused major changes in cell shape, including significant increases in cell diameter, which must require substantial cytoskeletal rearrangement. Peroxide-induced increases in cell diameter were, however, blocked by the selective proteasome inhibitor lactacystin. The degradation and resynthesis of ezrin may therefore be an underlying mechanism for overall cell shape changes observed during oxidative stress. Oxidative stress induces extensive protein oxidation and degradation and significant increases in cell blebbing, rounding-up, and overall size. Our results indicate that all these oxidant-induced changes may actually be catalyzed by the proteasome.—Grune, T., Reinheckel, T., North, J. A., Li, R., Bescos, P. B., Shringarpure, R., Davies, K. J. A. Ezrin turnover and cell shape changes catalyzed by proteasome in oxidatively stressed cells. *FASEB J.* 16, 1602–1610 (2002)**

Key Words: radixin · hydrogen peroxide · ezrin degradation · lactacystin · free radicals · proteolysis

CELLS UNDERGO MANY changes when exposed to oxidative stress. Severe oxidative stress can cause extreme results including loss of replicative capacity, senescence, and even cell death by either apoptosis or necrosis (1–3). In contrast, physiologically relevant exposure to oxidants causes much milder effects including shape changes (4), adaptive changes in gene expression (1, 2), and enzymatic repair and/or removal of oxidized cell components by DNA repair systems, lipases, and proteases (1–3).

Adherent cultured cells often react by blebbing, rounding-up, and detaching from the growth surface when treated with moderate levels of hydrogen peroxide (H_2O_2) (4). These changes indicate a major rearrangement of cytoskeletal proteins such as actin, ezrin, or filamin. In polymers, actin forms a rigid structure, providing the cell membrane with a scaffold on which to build, but it does not bind directly to the cell membrane. Filamin bundles actin filaments localized beneath the plasma membrane at cleavage furrows and stress fibers, but does not seem to directly anchor actin to the plasma membrane (5, 6). Ezrin, a constituent of the ezrin, radixin, and moesin family (ERM family) of proteins, binds actin (7, 8) and proteins in the lipid bilayer (8–10). Changes in cell morphology on oxidative stress could include detachment of cross-linker proteins such as ezrin from either the plasma membrane or the actin filament, or both.

Ezrin, radixin, and moesin contain binding sites for actin at their carboxyl termini and binding sites for transmembrane proteins such as intercellular adhesion molecules (ICAM) and CD44 at their amino-terminal end. Binding of the carboxyl end of ezrin to actin occurs in two distinct ways: indirect binding to the barbed (fast-growing) end of actin (11) and direct binding to the sides of actin filaments (7), suggesting different modes of cellular control for the actin superstructure. At the amino terminus, ezrin binding to ICAM is affected by other forms of stress such as viral infection. For example, in human fibroblasts infected with herpes simplex virus, ezrin was redistributed into newly formed microvilli with concomitant redistribution of ICAM into the nascent protrusions (12). These

[1] Current address: Departmento de Farmacologia, Universidad Complutense de Madrid.

[2] Senior and corresponding author: Ethel Percy Andrus Gerontology Center, 3715 McClintock Ave., Room 306, University of Southern California, Los Angeles, CA 90089-0191, USA. E-mail: kelvin@usc.edu

0892-6638/02/0016-1602 © FASEB

changes occurred without any apparent change in ezrin quantity, indicating that dynamic interactions between ezrin and cell shape changes are intimately controlled.

Although many studies show that oxidative stress results in protein damage and in the selective proteolysis of oxidatively modified proteins (13–51), very little is known about the fate of specific proteins that may be special targets of oxidative stress. The present study was designed to test for the existence of individual proteins that may undergo selective turnover after oxidative stress; after initial experiments, our work quickly focused on the fate of ezrin.

MATERIALS AND METHODS

Cells and cell culture

Clone 9 liver cells (normal rat liver epithelia) obtained from American Type Culture Collection (ATCC CRL 1439) were maintained in 90% Ham's F-12K medium supplemented with 10% fetal bovine serum, 2 mM L-glutamine, 10 Units/mL penicillin, and 10 μg/mL streptomycin. Cells were typically replated at a density of 2×10^4 cells/cm^2 every 2 or 3 days to maintain logarithmic growth. After experimental treatment, control cultures and treated samples were harvested using a tissue scraper and small amounts of cold phosphate-buffered saline (PBS) containing 1 mM EDTA. The cells were washed and resuspended in 300 μL PBS-EDTA in microcentrifuge tubes, disrupted by a 10 s burst of sonication (20 mW power), and the supernatant was collected after centrifugation for 15 min at 10,000 *g*. For electrophoresis and antibody studies, the homogenizing buffer contained a protease inhibitor mixture (Sigma catalog # P-8340) to decrease protein degradation during sample preparation.

Metabolic radiolabeling of cellular proteins

Cell cultures were washed with PBS and incubated for 2 h in Eagle's minimal essential medium without methionine or cysteine but containing 0.01 mCi/mL [^{35}S]-methionine/cysteine mixture (NEN catalog # NEG772). After cell proteins were metabolically radiolabeled, the cultures were washed twice with PBS and incubated with Ham's complete medium for 2 h as a cold "chase". These exact procedures have been used extensively in this laboratory for studies of protein turnover in various mammalian cells (22–29).

Exposure to oxidative stress

Subconfluent monolayers of clone 9 liver epithelial cells were exposed to bolus additions of H_2O_2. The amount of H_2O_2 used was corrected for the number of cells present in the culture so that in every experiment the concentration was normalized as μM H_2O_2 with 3×10^5 cells/cm^2 in a final exposure volume of 10 mL. After incubation at 37°C for 30 min, the cells were washed twice with PBS and harvested immediately (0 time point) or incubated with Ham's complete medium before washing and harvesting at the appropriate times.

2-D gel electrophoresis, Western blotting, and protein microsequencing

Two-dimensional polyacrylamide gel electrophoresis (2-D PAGE), the method originally described by O'Farrell (52) consisting of isoelectric focusing in the first dimension and sodium dodecyl sulfate (SDS) PAGE (10–12%) in the second dimension, was performed using a linear immobilized pH gradient from 4.0 to 7.0 (Pharmacia, Piscataway, NJ) as previously described (53). Western blots were visualized using several commercially available monoclonal antibodies directed against the carboxyl-terminal end of ezrin and an alkaline phosphatase-tagged secondary antibody. Amino-terminal protein microsequencing was performed using a 12% SDS-PAGE separating gel (16×20 cm) by electroblotting proteins onto PVDF membranes. Spots of particular interest were sent to Immuno-Dynamics (La Jolla, CA) for the actual protein sequencing.

RESULTS

Oxidative stress causes a proteasome-dependent increase in cellular proteolysis

Exposure of clone 9 liver cells to relatively low concentrations of H_2O_2 caused a sharp increase in overall cellular protein degradation, but higher concentrations progressively diminished proteolysis to below control levels (**Fig. 1**). Our previous studies indicate that proteolysis generally increases at lower H_2O_2 concentrations because mildly oxidized proteins are preferred proteolytic substrates (13–29). In contrast, heavily oxidized proteins (formed at high H_2O_2 exposures) form

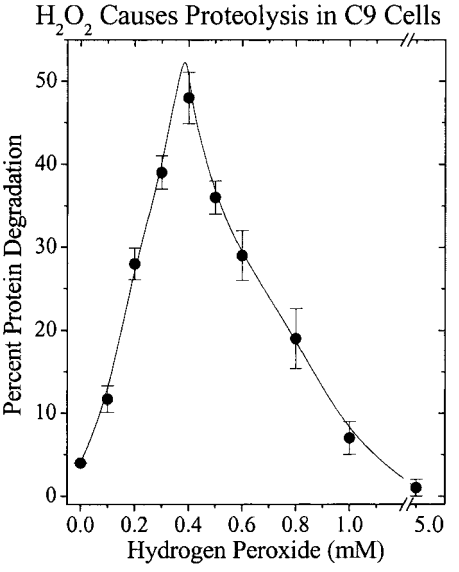

Figure 1. Hydrogen peroxide-induced protein degradation in clone 9 liver cells. Clone 9 liver cells (3×10^5 cells/cm^2 in a 10 mL reaction volume) containing metabolically ^{35}S-radiolabeled proteins were used as controls or exposed to concentrations of H_2O_2 ranging from 100 μM to 5.0 mM for 30 min at 37°C, as described in Materials and Methods. Overall protein degradation was measured by increases in acid-soluble radioactivity (reflecting the production of amino acids and small peptides from previously acid-insoluble, intact radiolabeled proteins) after cell disruption and trichloroacetic acid precipitation of remaining intact proteins, as described in detail in refs 22–29. Results shown are means and SE of three independent observations.

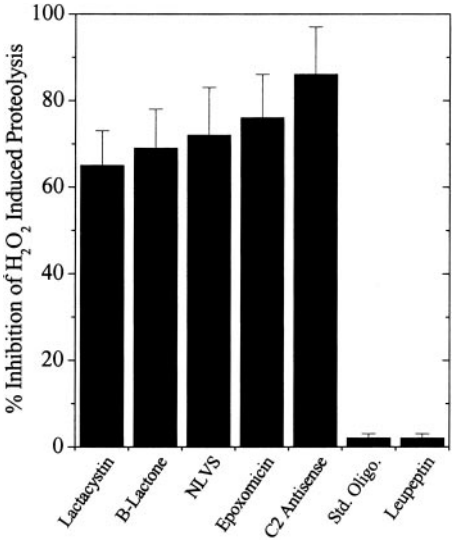

Figure 2. Inhibitors of hydrogen peroxide-induced proteolysis in clone 9 liver cells. Metabolically radiolabeled cells at 3×10^5 cells/cm^2 in a 10 mL reaction volume were exposed to 400 μM H_2O_2 for 30 min, as described in Fig. 1. The selective proteasome inhibitors lactacystin (10 μM), NLVS (tri-leucine vinyl sulfone; -t-Boc-GAR-MCA, *N*-t-Boc-Gln-Ala-Arg 7-amido-4-methylcoumarin at a concentration of 10 μM), epoxomycin (20 μM), or the lysosomal proteolysis inhibitor leupeptin (100 μM) were included in the incubation. In all cases the effects of DMSO vehicle alone, where used (always <5%), have been subtracted from the results shown. In some experiments, cells were preincubated for 7 days with daily 0.4 nmol/mL treatments of a proteasome C2 antisense morpholino-oligonucleotide (5′-AGCTATGTTTCGCAA-3′) or a standard (control) morpholino-oligonucleotide (both from GeneTools LLC) to decrease intracellular proteasome levels and activity, as described previously (22–29). Percent inhibition values shown above are expressed relative to the maximal proteolysis observed at 400 μM H_2O_2 in Fig. 1. All values are means and SE of four independent observations.

hydrophobic and ionic aggregates, as well as covalent cross-links, and therefore become progressively resistant to proteolysis (13–29, 47, 54).

Using exposure to 400 μM H_2O_2 with 3×10^5 cells/cm^2, which caused maximal proteolysis (Fig. 1), we next tested the effects of various proteolytic inhibitors (**Fig. 2**). The selective proteasome inhibitors lactacystin, β lactone, NLVS, and epoxomycin dramatically inhibited peroxide-induced proteolysis in clone 9 liver cells, as did specific lowering of intracellular proteasome levels by a 7-day pretreatment with an antisense oligonucleotide directed against the proteasome C-2 subunit (Fig. 2). Cell treatment with the proteasome C-2 antisense oligonucleotide lowered maximal proteasome activity by 87%, as judged by lactacystin-inhibitable degradation of the fluoropeptide substrate suc-LLVY-MCA, and caused >60% depletion of multiple proteasome subunits (presumably degraded due to inability to form complete complexes), in good agreement with previous work (22, 23; confirmatory electrophoretic data not shown). In contrast to these results implicating proteasome in H_2O_2-induced proteolysis, neither a standard, control oligonucleotide nor the lysosomal proteolysis inhibitor leupeptin had any significant effect (Fig. 2).

Selective degradation of three proteins during oxidative stress

Two-dimensional PAGE detected proteins undergoing selective degradation after exposure of clone 9 cells to H_2O_2. Three good examples include the "spots" labeled A, B, and C in the left panel of **Fig. 3**, which appear to be drastically diminished after oxidative stress, as shown in the right panel. To visualize this result, newly synthesized cell proteins were metabolically labeled by incorporation of [^{35}S]-methionine/cysteine before the 30 min H_2O_2 exposure. The loss of density of a radioactive protein "spot" after H_2O_2 stress indicates proteolytic degradation.

Protein "A" was not amenable to amino-terminal sequencing and protein "C" will be reported elsewhere (55). Protein "B" is the subject of the remainder of this paper. Protein B has an apparent molecular mass of 80 kDa and an acidic pI of ~ 6.0. This spot was excised from 2-D PAGE and the first 24 amino-terminal amino acids were microsequenced. A search of the SwissProt database by the BLASTP program revealed that the peptide sequence of our protein B from rat liver cells matched almost exactly the amino-terminal portion of

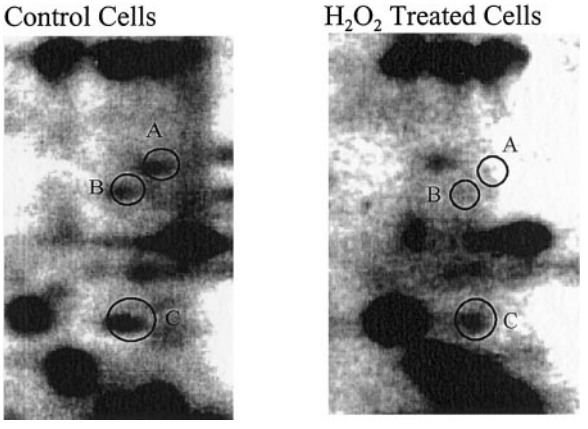

Figure 3. Oxidative stress causes degradation of at least three proteins in clone 9 liver cells. Partial 2-D polyacrylamide electrophoresis gels (showing the range of pH 5.5 to 6.5) of pre-radiolabeled proteins from clone 9 liver cells 24 h after exposure (right panel) or sham-exposure (left panel) to hydrogen peroxide. Intracellular proteins were metabolically radiolabeled with ^{35}S cysteine/methionine; cells at a density of 3×10^5 cells/cm^2 in a 10 mL reaction volume were exposed to 400 μM H_2O_2 (or used as controls), then disrupted and analyzed by 2-D electrophoresis, as described in Materials and Methods. The circled ^{35}S-radiolabeled protein spots labeled A, B, and C in both gels showed significant degradation 24 h post oxidative stress. The pH gradient becomes more basic to the right on the ordinate and the apparent molecular weight increases toward the top on the abscissa. Protein B had an apparent molecular mass of ~80,000 and an apparent PI of ~6.0 compared with standards. This figure represents one sample of at least 4 individual experiments, all of which produced very similar results.

the (bovine, human, and mouse) protein ezrin (56–70), a member of the ERM family of cytoskeleton membrane-anchoring proteins (56–74): ezrin, radixin, and moesin (**Table 1**).

We next used specific anti-ezrin antibodies to confirm the identity of protein B as ezrin, to carefully follow ezrin degradation, and to discriminated between ezrin, radixin, and moesin. Because of the extensive amino-terminal sequence homology between all the ERM proteins (56–74), antibodies directed against the carboxyl-terminal end of ezrin, radixin, and moesin were used to probe proteins transblotted onto membranes from 2-D PAGE gels. As shown in **Fig. 4**, The carboxyl-terminal anti-ezrin antibody highlighted a spot exactly corresponding to the 80 kDa, 6.0 PI radioactive spot previously observed to be preferentially degraded (Fig. 3). In a double-label experiment, the autoradiogram from a 2-D PAGE gel containing [^{35}S]-labeled proteins overlays directly with the Western results from the same blot Fig. 4). The radioactive spot tentatively identified by its amino-terminal sequence in Table 1 as ezrin is thus the same spot the carboxyl-terminal monoclonal antibody recognized as authentic ezrin in Fig. 4. Little interaction was observed between the protein B spot and either anti-radixin or anti-moesin carboxyl-terminal monoclonal antibodies (not shown). We were also able to reconfirm the identity of protein B as authentic ezrin by repeating the experiments of Fig. 4 using five other anti-ezrin carboxyl-terminal antibodies: catalog # sc-6409 from Santa Cruz Biotechnology (Santa Cruz, CA), catalog # sc-6407 from Santa Cruz Biotechnology (Santa Cruz, CA), catalog # 4398–8006 from ANAWA Biomedical Services & Products (Zurich, Switzerland), product # A 4700 from Sigma Chemical Co. (St. Louis, MO), and product # E 8897 from Sigma . These repeat experiments yielded results very similar to those reported in Fig. 4 (confirmatory data not shown) and provide greater confidence in the identification of protein B as ezrin.

Oxidative stress affects overall ezrin turnover

As shown in Fig. 3, when clone 9 liver cells are prelabeled with [^{35}S]-methionine/cysteine and exposed to H_2O_2, the radioactive spot on the 2-D PAGE gel corresponding to ezrin (protein B) diminishes. To assess possible gross changes in the intracellular steady-state content of ezrin, Western blots using carboxyl-terminal anti-ezrin monoclonal antibodies were performed. **Figure 5** shows no apparent change in the total amount of ezrin present over a 24 h period either in untreated control samples or with 3×10^5 cells/cm^2 exposed to 400 μM H_2O_2. This is consistent with other findings of unchanged steady-state protein concentrations after cellular exposures to stress (12). Control cells exhibited stable ezrin levels for at least 13 h in the presence of the protein synthesis inhibitor cycloheximide at 0.1 mg/mL (not shown). The results of Fig. 5 were repeated using the two Santa Cruz Biotechnology anti-ezrin carboxyl-terminal monoclonal antibodies (see above) with essentially identical results (data not shown). We next exposed cells to ^{35}S-labeled, newly synthesized proteins to 400 μM H_2O_2 and measured proteolysis by loss of radioactive ezrin counts, confirmed by Western blotting with a carboxyl-terminal anti-ezrin monoclonal antibody. As shown in the left panel of **Fig. 6**, H_2O_2 exposure caused a time-dependent degradation of ezrin in clone 9 liver cells.

Since radiolabeled (and presumably intact) ezrin was preferentially degraded on oxidative stress (Fig. 3 and Fig. 6, left panel), we reasoned that the maintenance of cellular levels of ezrin seen by Western analysis (Fig. 5) might be explained by increased synthesis of new ezrin molecules. Radiolabeling of proteins after peroxide exposure produces a snapshot of newly synthesized molecules. When unlabeled cells were first exposed to H_2O_2 and cellular proteins were then labeled with [^{35}S]-methionine/cysteine, a clear increase in the intensity of the ezrin spot (confirmed by Western blotting with the carboxyl-terminal anti-ezrin monoclonal antibody) was observed over time (Fig. 6, right panel). These changes in ezrin synthesis occurred as early as 3 h postperoxide treatment and persisted for up to 24 h. The increases observed in the intensities of radiolabeled ezrin after peroxide exposure indicate de novo synthesis of ezrin molecules. Taken with the results of Figs. 1–5, the data of Fig. 6 indicate that ezrin is preferentially degraded on H_2O_2 exposure and new ezrin is then synthesized.

TABLE 1. *Comparison of protein "B," ezrin, radixin, and moesin*

Peptide source	Sequence, amino terminus[a]	Homology (%) (# identical/24) × 100	Molecular mass (kDa)	Number of A.A. residues
Protein "B", rat clone 9	PKPINVRVTTMDAELEFAIQPNTS	–	80	–
Ezrin, bovine	PKPINVRVTTMDAELEFAIQPNTT (68)	96	80	581
Ezrin, human	PKPINVRVTTMDAELEFAIQPNTT (69)	96	83	586
Ezrin, mouse	PKPINVRVTTMDAELEFAIQPNTT (70)	96	85	586
Radixin, pig	PKPINVRVTTMDAELEFAIQPNTT (71)	96	82	583
Radixin, human	PKPINVRVTTMDAELEFAIQPNTT (72)	96	80	583
Moesin, rat	PKTISVRVTTMDAELEFAIQPNTT (73)	88	76	577
Moesin, human	PKTISVRVTTMDAELEFAIQPNTT (74)	88	75	577

[a] References for the amino-terminal sequences are shown in parentheses.

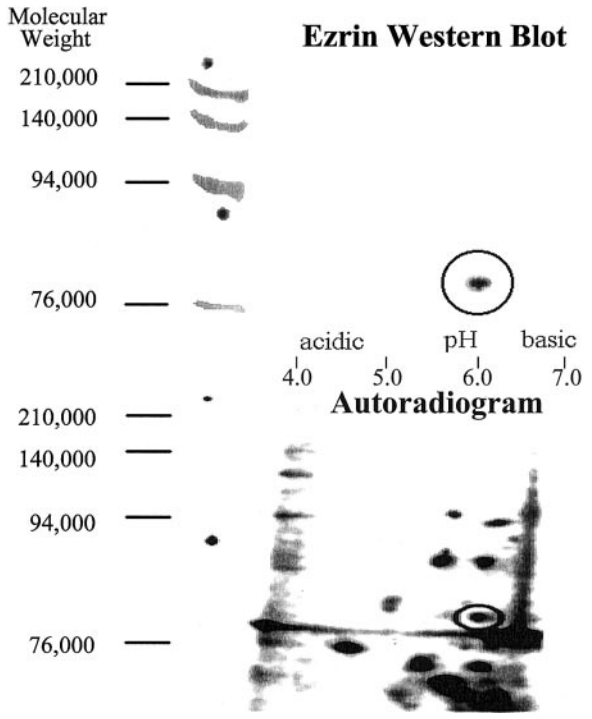

Figure 4. Comparison of Western blot analysis and 2-D PAGE autoradiography in identification of ezrin. Clone-9 liver cell proteins radiolabeled with [^{35}S]-methionine/cysteine were separated by 2-D PAGE gel electrophoresis, blotted onto a PVDF membrane and the membrane probed with monoclonal anti-ezrin antibody; results obtained are shown in the top panel. Western blots were visualized using a primary monoclonal goat anti human antibody directed against the carboxyl-terminal end of ezrin (catalog # E13420, Transduction Laboratories, Lexington, KY) and an alkaline phosphatase-tagged secondary antibody (catalog # A2556, Sigma). The same membrane was then used to produce the autoradiogram seen in the bottom panel. In the molecular weight marker lane radioactive dots were placed on the membrane for reference during analysis. The single spot highlighted by the circle on the Western blot corresponds exactly with the spot highlighted by the circle on the autoradiogram. These results were repeated three times with essentially identical results.

Ezrin degradation and cell shape changes are catalyzed by proteasome

Since ezrin appears to undergo oxidant-induced proteolysis and overall increases in oxidant-induced cellular protein degradation appear to be largely catalyzed by the proteasome (Fig. 2; 16–29, 75), we wanted to know whether proteasome is also responsible for ezrin breakdown. Using the same proteasome inhibitors and C2 subunit antisense oligonucleotides as in Fig. 2, we were able to selectively inhibit H_2O_2-induced ezrin degradation by an average of 72–90% (**Fig. 7**). These results indicate that proteasome is responsible for most ezrin degradation after oxidative stress.

As described earlier, oxidative stress induces extensive protein oxidation and degradation (13–51) and significant increases in cell blebbing, rounding-up, and overall size (4, 53). The results of Figs. 1–7 indicate that all these oxidant-induced changes may actually be catalyzed by the proteasome. To test this hypothesis, we measured H_2O_2-induced increases in clone 9 cell size in the presence and absence of the proteasome inhibitor lactacystin (**Fig. 8**). Our data show a clear and reproducible increase in cell size with H_2O_2 treatment, which was inhibited by almost 70% in the presence of lactacystin (Fig. 8), indicating a major proteasome involvement in oxidant-induced cell shape changes. We have also observed similar results in K562 erythroleukemia cells (confirmatory data not shown).

DISCUSSION

We now report that during oxidant-induced increases in overall cellular proteolysis, the cytoskeletal-anchoring protein ezrin is one of the main cytoplasmic proteins to be degraded. Since the proteasome is largely

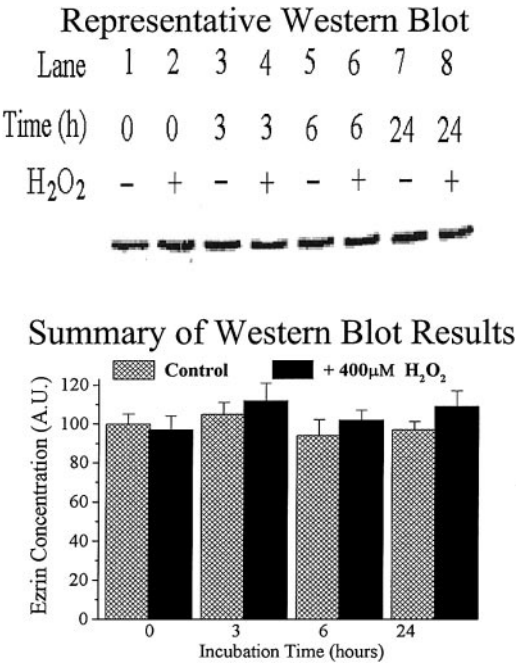

Figure 5. Western blot analysis of steady-state ezrin levels after hydrogen peroxide treatment. Clone 9 liver cells exposed to hydrogen peroxide (400 μM H_2O_2 with 3×10^5 cells/cm^2 in a 10 mL reaction volume) were harvested at the times shown. After electrophoresis by denaturing 10% SDS-PAGE, cellular proteins were transblotted onto a PVDF membrane. Ezrin was visualized using a primary monoclonal goat anti human antibody directed against the carboxyl-terminal end of ezrin (catalog # E13420, Transduction Laboratories) and an alkaline phosphatase-tagged secondary antibody (catalog # A2556, Sigma). The upper panel shows a single SDS-PAGE (representative Western blot); the lower panel (summary of Western blot results) describes a summary of six independent experiments in which ezrin levels were quantified by densitometry and are expressed in arbitrary units (A.U.) relative to the zero time control cells, which are set at 100 A.U. All values are means and SE.

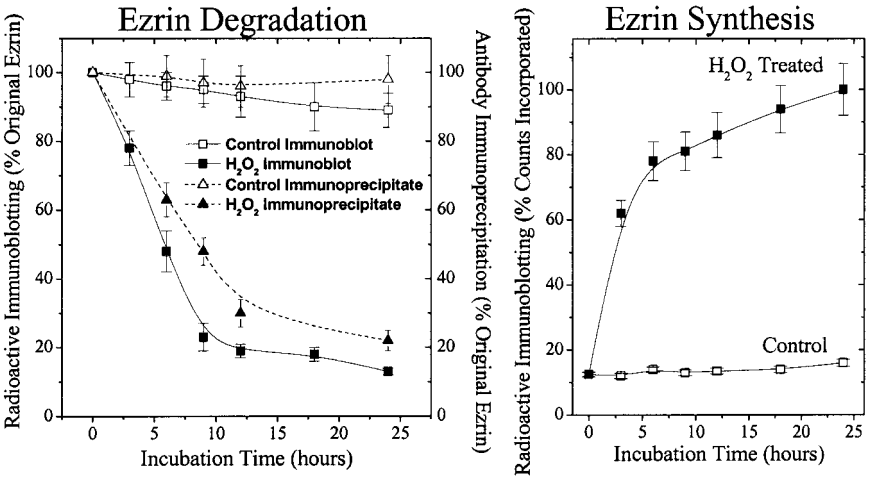

Figure 6. Ezrin turnover induced by hydrogen peroxide in clone 9 liver cells. To measure ezrin degradation (right panel), cell proteins were first metabolically radiolabeled with ^{35}S-cysteine/methionine, then exposed to 400 μM H_2O_2 (using 3×10^5 cells/cm^2 in a 10 mL reaction volume) for 30 min at 37°C as per Fig. 3. To measure ezrin protein synthesis (right panel) cells were exposed to 400 μM H_2O_2, then cell proteins were metabolically radiolabeled with ^{35}S-cysteine/methionine. Ezrin degradation or synthesis was measured by quantifying the radioactivity in 2-D gel electrophoresis spots, whose identity was confirmed by immunoblotting with a monoclonal antibody directed against the ezrin COOH terminus (see Figs. 4 and 5). All values shown are means and SE of at least 3 independent observations.

responsible for oxidant-induced intracellular proteolysis (24, 75), we wanted to know whether proteasome is also responsible for ezrin breakdown. Using proteasome inhibitors and proteasome C2 subunit antisense oligonucleotides, we were able to selectively inhibit H_2O_2-induced ezrin degradation by an average of 72–90%. These results indicate that proteasome is responsible for most ezrin degradation after oxidative stress. Whether ezrin undergoes oxidative modification to become a substrate for proteasome proteolysis or whether H_2O_2 initiates a signal transduction pathway that results in global degradation of cellular ezrin by proteasome is not yet clear. Oxidative stress causes significant cell blebbing and rounding-up, which (initially) result in increased cell size (4, 53) . Our results show that lactacystin can inhibit this oxidant-induced increase in cell size by up to 70% (Fig. 7), indicating that by degrading ezrin anchors between the cytoskeleton and the cell membrane, proteasome can play a major role in oxidant-induced cell shape changes.

The cytoskeleton appears static, but in reality synthesis and degradation of component proteins occur continuously. Cell shape and membrane composition respond to extracellular pressures and signals, especially the transport, nucleation, polymerization, and capping

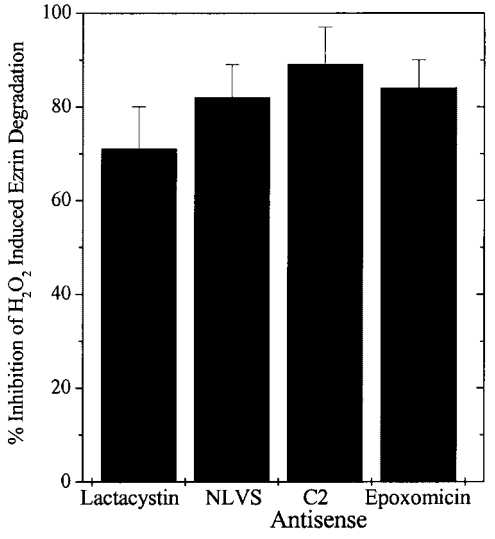

Figure 7. Proteasome inhibitors block hydrogen peroxide-induced ezrin degradation in clone 9 liver cells. Ezrin degradation was measured as described in the legend to Fig. 6 (left panel) after exposure of cells at a density of 3×10^5 cells/cm^2 in a 10 mL reaction volume to 400 μM H_2O_2 for 30 min at 37°C. Effects of various protease inhibitors and proteasome C2 subunit antisense morpholino-oligonucleotides were tested exactly as described in the legend to Fig. 2. A standard (control) morpholono-oligonucleotide was tested (as per Fig. 2) and found to have no effect (data not shown). Values shown are the means and SE of 3 independent observations.

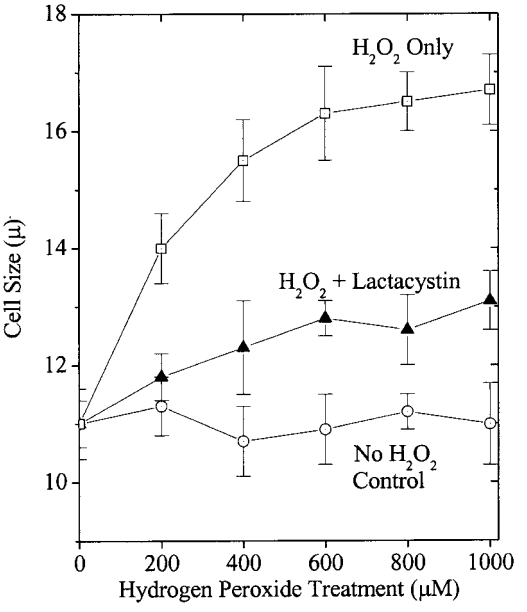

Figure 8. Proteasome-dependent increases in clone 9 liver cell size induced by hydrogen peroxide. Cells (at a density of 3×10^5 cells/cm^2 in a 10 mL reaction volume) were used as controls or exposed to 200 μM to 1.0 mM H_2O_2 at 37°C in the presence or absence of 10 μM lactacystin. After 5 h of incubation, cell size was measured using a Coulter counter. Lactacystin had no effect on cell size in control samples not exposed to H_2O_2 (data not shown). Values shown are the means and SE of 3 independent observations.

of actin fibers, an integral part of the cytoskeleton. Ezrin, a cytoskeletal protein that anchors actin polymers to the lipid bilayer, represents a class of regulatory proteins that can provide exquisite control of actin activity and cytoskeletal rearrangements. Ezrin is found in high concentrations at the growing edges of cells (pseudopodia) and in cell structures that require rapid mobilization and relocation of actin fibers—for example, microvilli (6, 56–58). These structures need Ezrin to bind to actin fibers, regulate actin polymerization, and cap growing actin filaments (7, 8, 59). The presence of this length-regulating mechanism through ezrin provides the cell with a means of handling responses to extracellular conditions.

For actin filaments to serve as mobile structural girders of the cytoskeleton that can allow changes in cell shape, they must be released from the membrane and relocated. This can be accomplished by degrading actin, then synthesizing new actin polymers and transporting them to the relocation site. Alternatively, intact actin can be released by removing its ezrin anchor. Free actin fibers can then be relocated and the new ezrin anchors synthesized. Our results show that ezrin is preferentially degraded by the proteasome after exposure to oxidative stress. Equally important, de novo synthesis of ezrin immediately follows oxidative stress. Our finding that de novo synthesis of ezrin increases despite no change in overall amount of ezrin after oxidative stress is similar to results observed by ourselves and by others (8, 12) after viral infection. This would indicate that the turnover of ezrin is linked directly to a cellular sensor that determines when and where the cell needs to reposition its cytoskeleton. No increase in the cell content of ezrin should be required for the cell shape changes w, and others (4, 53) have observed with oxidative stress. Instead, the breaking of existing ezrin bridges between the cytoskeleton and the cell membrane (by proteasome), followed by synthesis of new ezrin molecules that attach the cytoskeleton and the membrane in a new configuration allowing for rounding-up and blebbing, is proposed.

Ezrin is dissociated from the cytoskeleton by anoxia and by epidermal growth factor (60, 61). Oxidative stress can now be added to the list of conditions that affect ezrin/cytoskeleton interactions. Hydrogen peroxide exposure of adherent cells causes significant increases in cell diameter, rounding-up, and lifting of the cells from the supporting tissue culture flask (4, 53). This process may involve the severing of ezrin from identified adhesion molecules or other proteins that facilitate extracellular in vitro adhesion. Interactions between ezrin and intercellular adhesion molecules as well as surface proteins have been reported (62–64). Subsequent redistribution of these molecules could serve to help protect cells from the cytotoxic effects of oxidative stress. Redistribution of ezrin has been observed after infection of human fibroblasts with herpes virus (8, 12). Our results indicate that ezrin is a prime candidate for the mobilization of actin in response to stress and for cell shape changes that result from oxidative stress. FJ

This research was supported by National Institutes of Health/NIEHS grant ES-03598 to K.J.A.D.

REFERENCES

1. Davies, K. J. A. (1995) Oxidative stress: the paradox of aerobic life. *Biochem. Soc. Symp.* **61,** 1–31
2. Davies, K. J. A. (1999) The broad spectrum of responses to oxidants in proliferating cells: a new paradigm for oxidative stress. *IUBMB Life* **48,** 41–47
3. Davies, K. J. A. (2000) Oxidative stress, antioxidant defenses, and damage removal, repair, and replacement systems. *IUBMB Life* **50,** 35–41
4. Bellomo, G., Jewell, S. A., Thor, H., and Orrenius, S. (1982) Regulation of intracellular calcium compartmentation: studies with isolated hepatocytes and t-butyl hydroperoxide. *Proc. Natl. Acad. Sci. USA* **79,** 6842–6846
5. Tsukita, S., Yonemura, S., and Tsukita, S. (1977) ERM proteins: head-to-tail regulation of actin-plasma membrane interaction. *Trends Biochem. Sci.* **22,** 53–58
6. Geiger, B., Avnur, Z., Rinnerthaler, G., Hansen, H., and Small, V. J. (1984) Microfilament-organizing centers in areas of cell contact: cytoskeletal interactions during cell attachment and locomotion. *J. Cell Biol.* **99,** 83S–91S.
7. Yak, X., Cheng, L., and Forte, J. G. (1996) Biochemical characterization of ezrin-actin interaction. *J. Biol. Chem.* **271,** 7224–7229
8. Vaheri, A., Carpen, O., Heiska, L., Helander, T. S., Jaaskelainen, J., Majander-Nordenswan, P., Sainio, M., Timonen, T., and Turunen, O. (1997) The ezrin protein family: membrane-cytoskeleton interactions and disease associations. *Curr. Opin. Cell Biol.* **9,** 659–666
9. Turunen, O., Wahlstrom, T., and Vaheri, A. (1994) Ezrin has a COOH-terminal actin-binding site that is conserved in the ezrin protein family. *J. Cell Biol.* **126,** 1445–1453
10. Pestonjamasp, K., Amieva, M. R., Strassel, C. P., Nauseef, W. M., Furthmayr, H., and Luna, E. J. (1995) Moesin, ezrin, and p205 are actin-binding proteins associated with neutrophil plasma membranes. *Mol. Biol. Cell* **6,** 247–259
11. Shuster, C. B., Lin, A. Y., Nayak, R., and Herman, I. M. (1996) bCAP73: a novel β actin-specific binding protein. *Cell Motil. Cytoskel.* **354,** 175–187
12. Pakkanen, R., von Bonsdorff, C-H., Turunen, O., Wahlstrom, T., and Vaheri, A. (1988) Redistribution of M_r 75000 plasma membrane protein, cytovillin, into newly formed microvilli in herpes simplex and Semliki Forest virus infected human embryonal fibroblasts. *Eur. J. Cell Biol.* **46,** 435–443
13. Davies, K. J. A. (1986) Intracellular proteolytic systems may function as secondary antioxidant defenses: an hypothesis. *Free Radic. Biol. Med.* **2,** 155–173
14. Davies, K. J. A., and Goldberg, A. L. (1987) Proteins damaged by oxygen radicals are rapidly degraded in extracts of red blood cells. *J. Biol. Chem.* **262,** 8227–8234
15. Davies, K. J. A., Lin, S. W., and Pacifici, R. E. (1987) Protein damage and degradation by oxygen radicals: IV. Degradation of denatured protein. *J. Biol. Chem.* **262,** 9914–9920
16. Pacifici, R. E., Salo, D. C., Lin, S. W., and Davies, K. J. A. (1989) Macroxyproteinase (M.O.P.): A 670 kDa proteinase complex that degrades oxidatively denatured proteins in red blood cells. *Free Radic. Biol. Med.* **7,** 521–536
17. Salo, D. C., Pacifici, R. E., and Davies, K. J. A. (1990) Superoxide dismutase undergoes proteolysis and fragmentation following oxidative modification and inactivation. *J. Biol. Chem.* **265,** 11919–11927
18. Giulivi, C., and Davies, K. J. A. (1993) Dityrosine and tyrosine oxidation products are endogenous markers for the selective proteolysis of oxidatively modified red blood cell hemoglobin by the (19 S) proteasome *J. Biol. Chem.* **268,** 8752–8759

19. Davies, K. J. A. (1993) Protein modification by oxidants and the role of proteolytic enzymes. *Biochem. Soc. Trans.* **21,** 346–353
20. Pacifici, R. E., Kono, Y., and Davies, K. J. A. (1993) Hydrophobicity as the signal for selective degradation of hydroxyl radical modified hemoglobin by the multicatalytic proteinase complex, proteasome. *J. Biol. Chem.* **268,** 15405–15411
21. Giulivi, C., Pacifici, R. E., and Davies, K. J. A. (1994) Exposure of hydrophobic moieties promotes the selective degradation of hydrogen peroxide-modified hemoglobin by the multicatalytic proteinase complex, proteasome. *Arch. Biochem. Biophys.* **311,** 329–341
22. Grune, T., Reinheckel, T., and Davies, K. J. A. (1995) Protein degradation in cultured liver epithelial cells during oxidative stress: role of the multicatalytic proteinase complex, proteasome. *J. Biol. Chem.* **270,** 2344–2351
23. Grune, T., Reinheckel, T., and Davies, K. J. A. (1996) Degradation of oxidized proteins in K562 human K-562 hematopoietic cells by proteasome. *J. Biol. Chem.* **271,** 15504–15509
24. Grune, T., Reinheckel, T., and Davies, K. J. A. (1997) Degradation of oxidized proteins in mammalian cells. *FASEB J.* **11,** 526–534
25. Grune, T., Blasig, I. E., Sitte, N., Roloff, B., Haseloff, R., and Davies, K. J. A. (1998) Peroxynitrite increases the degradation of aconitase and other cellular proteins by proteasome. *J. Biol. Chem.* **273,** 10857–10862
26. Ullrich, O., Reinheckel, T., Sitte, N., Haass, G., Grune, T., and Davies, K. J. A. (1999) Poly-ADP-ribose-polymerase activates nuclear proteasome to degrade oxidatively damaged histones. *Proc. Natl. Acad. Sci. USA* **96,** 6223–6228
27. Sitte, N., Huber, M., Grune, T., Ladhoff, A., Doecke, W.-D., von Zglinicki, T., and Davies, K. J. A., (2000). Proteasome inhibition by lipofuscin/ceroid during postmitotic aging of fibroblasts. *FASEB J.* **14,** 1490–1498
28. Sitte, N., Merker, K., von Zglinicki, T., Grune, T., and Davies, K. J. A. (2000) Protein oxidation and degradation during cellular senescence of BJ fibroblasts: part I—effects of proliferative senescence. *FASEB J.* **14,** 2495–2502
29. Sitte, N., Merker, K., von Zglinicki, T., Davies, K. J. A., and Grune, T. (2000) Protein oxidation and degradation during cellular senescence of BJ fibroblasts: part II—aging of nondividing cells. *FASEB J.* **14,** 2503–2510
30. Levine, R. L., Oliver, C. N., Fulks, R. M., and Stadtman, E. R. (1981) Turnover of bacterial glutamine synthetase: oxidative inactivation precedes proteolysis. *Proc. Natl. Acad. Sci. USA* **78,** 2120–2124
31. Fucci, L., Oliver, C. N., Coon, M. J., and Stadtman, E. R. (1983) Inactivation of key metabolic enzymes by mixed function oxidation reactions: possible implication in protein turnover and aging. *Proc. Natl. Acad. Sci. USA* **80,** 1521–1525
32. Rivett, J. A. (1985) Preferential degradation of the oxidatively modified form of glutamine synthetase by intracellular mammalian proteases. *J. Biol. Chem.* **260,** 300–305
33. Rivett, J. A. (1985) Purification of a liver alkaline protease which degrades oxidatively modified glutamine synthetase. Characterization as a high molecular weight cysteine protease. *J. Biol. Chem.* **260,** 12600–12606
34. Stadtman, E. R. (1986) Oxidation of proteins by mixed-function oxidation system: Implication in protein turnover, ageing, and neutrophil function. *Trends Biochem. Sci.* **11,** 11–12
35. Oliver, C. N. (1987) Inactivation of enzymes and modification of proteins by stimulated neutrophils. *Arch. Biochem. Biophys.* **253,** 62–72
36. Oliver, C. N., Ahn, B., Moerman, E. J., Goldstein, S., and Stadtman, E. R. (1987) Age-related changes in oxidized proteins. *J. Biol. Chem.* **262,** 5488–5491
37. Oliver, C. N., Levine, R. L., and Stadtman, E. R. (1987) A role of mixed-function oxidation of altered enzyme forms during aging. *J. Am. Geriatr. Soc.* **35,** 947–956
38. Cervera, J., and Levine, R. L. (1988) Modulation of the hydrophobicity of glutamine synthetase by mixed-function oxidation. *FASEB J.* **2,** 2591–2595
39. Starke-Reed, P. E., and Oliver, C. N. (1989) Protein oxidation and proteolysis during aging and oxidative stress. *Arch. Biochem. Biophys.* **275,** 559–567
40. Levine, R. L., Garland, D., Oliver, C. N., Amici, A., Climent, I., Lenz A-G, Ahn, B., Shaltiel, S., and Stadtman, E. R. (1990) Determination of carbonyl content in oxidatively modified proteins. *Methods Enzymol.* **186,** 464–478
41. Stadtman, E. R., and Oliver, C. N. (1991) Metal-catalyzed oxidation of proteins: Physiological consequences. *J. Biol. Chem.* **266,** 2005–2008
42. Szweda, L. I., and Stadtman, E. R. (1992) Iron-catalyzed oxidative modification of glucose-6-phosphate dehydrogenase from *Leuconostoc mesenteroides*: structural and functional changes. *J. Biol. Chem.* **267,** 3096–3100
43. Stadtman, E. R. (1993) Oxidation of free amino acids and amino acid residues in proteins by radiolysis and by metal-catalyzed reactions. *Annu. Rev. Biochem.* **62,** 797–821
44. Levine, R. L., Mosoni, L., Berlett, B. S., and Stadtman, E. R. (1996) Methionine residues as endogenous antioxidants in proteins. *Proc. Natl. Acad. Sci. USA* **93,** 15036–1504045
45. Berlett, B. S., and Stadtman, E. R. (1997) Protein oxidation in aging, disease, and oxidative stress. *J. Biol. Chem.* **272,** 20313–20316
46. Chao, C.-C., Ma, Y.-S., and Stadtman, E. R. (1997) Modification of protein surface hydrophobicity and methionine oxidation by oxidative systems. *Proc. Natl. Acad. Sci. USA* **94,** 2969–2974
47. Taylor, A., and Davies, K. J. A. (1987) Protein oxidation and diminished proteolytic capacity in cataract formation during aging. *Free Radic. Biol. Med.* **3,** 371–377
48. Murakami, K., Jahngen, J. H., Lin, S. W., Davies, K. J. A., and Taylor, A. (1990) Degradation of eye lens alpha-crystallin by a lens high molecular weight proteinase following exposure to hydroxyl radicals. *Free Radic. Biol. Med.* **8,** 217–222
49. Huang, L. L., Shang, F., Nowell, T. R., Jr., and Taylor, A. (1995) Degradation of differentially oxidized alpha-crystallins in bovine lens epithelial cells. *Exp. Eye Res.* **61,** 45–54
50. Guo, B., Phillips, J. D., Yu, Y., and Leibold, E. A. (1995) Iron regulates the intracellular degradation of iron regulatory protein 2 by the proteasome. *J. Biol. Chem.* **270,** 21645–21651
51. Wolff, S. P., Garner, A., and Dean, R. T. (1986) Free radicals, lipids, and protein degradation. *Trends Biochem. Sci.* **11,** 27–31
52. O'Farrell, P. H. (1975) High resolution two-dimensional electrophoresis of proteins. *J. Biol. Chem.* **250,** 4007–4021
53. Wiese, A. G., Pacifici, R. E., and Davies, K. J. A. (1995) Transient adaptation to oxidative stress in mammalian cells. *Arch. Biochem. Biophys.* **318,** 231–240
54. Dean, R. T., Thomas, S. M., and Garner, A. (1986) Free-radical-mediated fragmentation of monoamine oxidase in the mitochondrial membrane. *Biochem. J.* **240,** 489–494
55. Grune, T., Reinheckel, T., Li, R., North, J. A., and Davies, K. J. A. (2002) Proteasome-dependent turnover of protein disulfide isomerase in oxidatively stressed cells. *Arch. Biochem. Biophys.* **397,** 407–413
56. Birgbauer, E., Dinsmore, J. H., Winckler, B., Lander, A. D., and Solomon, F. (1991) Association of ezrin isoforms with the neuronal cytoskeleton. *J. Neurosci. Res.* **30,** 232–241
57. Berryman, M., Franck, Z., and Bretscher, A. (1993) Ezrin is concentrated in the apical microvilli of a wide variety of epithelial cells whereas moesin is found primarily in endothelial cells. *J. Cell Sci.* **105,** 1025–1043
58. Stidwell, R. P., Wysolmerski, T., and Burgess, D. R. (1984) The brush border cytoskeleton is not static: In vivo turnover of proteins. *J. Cell Biol.* **98,** 641–645
59. Sato, N., Funayama, N., Nagafuchi, A., Yonemura, S., Tsukita, S., and Tsukita, S. (1992) A gene family consisting of ezrin, radixin and moesin. Its specific localization at actin filament/plasma membrane association sites. *J. Cell Sci.* **103,** 131–143
60. Bretscher, A. (1989) Rapid phosphorylation and reorganization of ezrin and spectrin accompany morphological changes induced in A-431 cells by epidermal growth factor. *J. Cell Biol.* **108,** 921–930
61. Chen, J., Doctor, B. R., and Mandel, L. J. (1994) Cytoskeletal dissociation of ezrin during renal anoxia: role in microvillar injury. *Am. J. Physiol.* **267,** C784–C795
62. Helander, T. S., Carpen, O., Turunen, O., Kovanen, P. E., Vaheri, A., and Timonen, T. (1996) ICAM-2 redistributed by ezrin as a target for killer cells. *Nature (London)* **382,** 265–268
63. Tsukita, S., Oishi, K., Sato, N., Sagara, J., Kawai, A., and Tsukita, S. (1994) ERM family members as molecular linkers between the cell surface glycoprotein CD44 and actin-based cytoskeletons. *J. Cell Biol.* **126,** 391–401

64. Lamb, R. F., Ozanne, B. W., Roy, C., McGarry, L., Stipp, C., Mangeat, P., and Jay, D. G. (1997) Essential functions of ezrin in maintenance of cell shape and lamellipodial extension in normal and transformed fibroblasts *Curr. Biol.* **7**, 682–688
65. Joos, K., and Muller, R. (1995) Deregulation of genes encoding microfilament-associated proteins during Fos-induced morphological transformation. *Oncogene* **10,** 603–608
66. Barila, D., Murgia, C., Nobili, F., and Perozzi, G. (1995) Transcriptional regulation of the ezrin gene during rat intestinal development and epithelial differentiation. *Biochim. Biophys. Acta* **1263,** 133–140
67. Cowell, G. M., and Danielsen, E. M. (1984) Biosynthesis of intestinal microvillar proteins. *FEBS Lett.* **172,** 309–314
68. Bergson, C. M., Zhao, H., Saijoh, K., Duman, R. S., and Nestler, E. J. (1993) Ezrin and osteonectin, two proteins associated with cell shape and growth, are enriched in the locus coeruleus. *Mol. Cell. Neurosci.* **4,** 64–73
69. Bauw, G., Rasmussen, H. H., van den Bulcke, M., van Damme, J., Puype, M., Gesser, B., Celis, J. E., and Vandekerckhove, J. (1990) Two-dimensional gel electrophoresis, protein electroblotting and microsequencing: a direct link between proteins and genes. *Electrophoresis* **11,** 528–536
70. Funayama, N., Nagafuchi, A., Sato, N., Tsukita, S, and Tsukita, S. (1991) Radixin is a novel member of the band 4.1 family. *J. Cell Biol.* **115,** 1039–1048
71. Lankes, W. T., Schwartz-Albiez, R, and Furthmayr, H. (1993) Cloning and sequencing of porcine moesin and radixin cDNA and identification of highly conserved domains. *Biochim. Biophys. Acta* **1216,** 479–482
72. Wilgenbus, K. K., Milatovich, A., Francke, U., and Furthmayr, H. (1993) Molecular cloning, cDNA sequence, and chromosomal assignment of the human radixin gene and two dispersed pseudogenes *Genomics* **16,** 199–206
73. Wang, L., Pang, X., Wang, Y., and Theoharides, T. C. Association of rat mast cell moesin with cellular proteins. Unpublished, direct submission to the GENBANK database, accession AF004811
74. Lankes, W. T., and Furthmayr, H. (1991) Moesin: a member of the protein 4.1-talin-ezrin family of protein. *Proc. Natl. Acad. Sci. USA* **88,** 8297–8301
75. Davies, K. J. A. (2001) Degradation of oxidized proteins by the 20S proteasome. *Biochimie (Paris)* **83,** 301–310

Received for publication January 28, 2002.
Accepted for publication June 23, 2002.